Available online at www.sciencedirect.com

ScienceDirect

IFAC Papers Online CONFERENCE PAPER ARCHIVE

IFAC-PapersOnLine 49-13 (2016) 076–081

Continuous compliance compensation of position-dependent flexible structures

Nikolaos Kontaras * **Marcel Heertjes** ** **Hans Zwart** ***

* *Control Systems Technology group, Eindhoven University of Technology, The Netherlands, (e-mail: n.kontaras@tue.nl).*
** *ASML, Mechatronic System Development, Veldhoven, The Netherlands, and Control Systems Technology group, Eindhoven University of Technology, The Netherlands, (e-mail: marcel.heertjes@asml.com, m.f.heertjes@tue.nl)*
*** *Department of Applied Mathematics, University of Twente, The Netherlands, and Dynamics and Control group, Eindhoven University of Technology, The Netherlands, (e-mail: h.j.zwart@utwente.nl, h.j.zwart@tue.nl)*

Abstract:
The implementation of lightweight high-performance motion systems in lithography and other applications imposes lower requirements on actuators, amplifiers, and cooling. However, the decreased stiffness of lightweight designs increases the effect of structural flexibilities especially when the point of interest is not at a fixed location. This is for example occurring when exposing a silicon wafer. The present work addresses the problem of compliance compensation in flexible structures, when the performance location is time-varying. The compliance function is derived using the frequency domain representation of the solution of the partial differential equation (PDE) describing the structure. The method is validated by simulation results.

Keywords: partial differential equation, PDE, flexible structures, Euler-Bernoulli beam, feedforward, compliance compensation.

1. INTRODUCTION

In the semiconductor industry, the focus on ever improving throughput, overlay, and imaging of exposed silicon wafers traditionally lead to more aggressive motion profiles, i.e. higher accelerations, and structural designs with higher stiffness and mass. The required forces to be applied during operation are therefore higher, and thus increasing the demands on actuators, amplifiers, and cooling. The resulting force density and heat generation necessitated to accelerate the mass therefore becomes increasingly infeasible, which prompts for a paradigm shift toward more flexible lightweight designs. As a consequence, when the performance location changes with time during wafer exposure, the dynamics of the system change due to significant contributions from structural modes. This leads to the requirement of taking the time-varying aspect of the plant into account when calculating feedforward compensation forces, which are key in achieving position accuracy.

The traditional approach toward the positioning problem would be an acceleration (or mass) feedforward controller, but this is not sufficient to compensate for flexible dynamics. Moreover, snap feedforward control (Boerlage (2006)) can only account for structural flexibilities to a certain extend. Namely, it cannot cope easily with time or parameter varying dynamics. Iterative learning control (ILC) (Dijkstra (2004)), (van de Wijdeven (2008)), which exploits a converged feedforward signal (rather than a filter) using the measured error from consecutive experiments, has the limitation of being setpoint trajectory dependent. Additionaly, ILC is not likely to take the exact plant variation with respect to time into account, but can possibly use an uncertainty model to encapsulate this instead. More recently, spatial feedforward control (Ronde et al. (2012)) has been developed in order to prevent excitation of the structural modes of the positioning system. However this method uses over-actuation. Hence, the output of structural modes to be suppressed should equal the amount of additional actuators. Inferential motion control has been opted to tackle the problem of taking into account position-dependent dynamics (Oomen et al. (2015)), however with limitations, e.g. a fixed point-of-interest, and not yet in a feedforward framework. In Sato (2003) a method is presented to design a gain-scheduled inverse of a Linear Parameter-Varying (LPV) system. For this method, an infinite number of Linear Matrix Inequalities (LMIs) has to be solved, which poses a challenge. This issue is solved in Sato (2008), however, the solution is based on LMI formulations, which do not always render feasible solutions in the case of high-order industrial systems. In (Ronde et al. (2013)), the work closest to compliance compensation presented here, a feedforward method for flexible systems with time-varying performance locations is presented. The method utilizes a lifted feedforward (discrete-time) representation, however, it does not take the manner of plant variation in-between the time-intervals into account.

10.1016/j.ifacol.2016.07.930

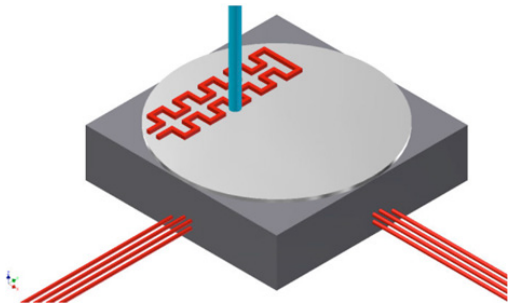

Fig. 1. Wafer stage of a lithographic system, where the sensors lie at the edges of the stage. During exposure of the silicon wafer to the laser beam, the performance location changes in time.

The contribution of this work is twofold. First, a position-dependent compliance compensation method is introduced, which accounts for the compliant part of the structural dynamics in the motion system. This is an extension of the work in Vervoordeldonk, Baggen (2009), and includes cases with a time-varying performance location such as occurring during wafer exposure. Secondly, the spatially continuous dynamics of the flexible structure (simplified by an Euler-Bernoulli beam) are derived from a partial differential equation (PDE). The PDE representation is exploited to derive the position-dependent compliance function of the beam. The method is validated by continuous-time simulation, using a simulation model containing a single structural mode, which is corrected to obtain the compliance of the original infinite-dimensional model.

The remainder of this paper is organized as follows. Section 2 introduces the compliance compensation control scheme and problem statement. Section 3 extends the compliance compensation concept to position-dependent distributed parameter systems with time-varying performance locations. Section 4 discusses the simulation environment and the results which validate the method. Finally, in Section 5, some concluding remarks are given.

2. PROBLEM STATEMENT

During the production of chips, a silicon wafer is positioned atop the wafer stage of the lithographic system. A source emanating (extreme) ultraviolet (EUV) light passes through the reticle, which is part of the reticle stage, and which contains a blueprint of the integrated circuits (ICs) to be processed. Beyond the reticle, light passes an optical system with controlled mirrors before it exposes the photo-sensitive layers of the wafer's surface. An illustration of the wafer stage during exposure is shown in Fig. 1. Assuming that it is a lightweight structure, i.e. its dynamics are substantially dependent on position, it follows that during exposure the time-varying performance location is subjected to position-dependent dynamics.

In light of these position-dependent dynamics, the compliance compensation method will be considered for infinite-dimensional flexible structures in Section 3 (see Vervoordeldonk, Baggen (2009)). In this section, the concept of compliance compensation is explained for the static output case only.

The block diagram of the proposed control scheme is given in Fig. 2, and consists of the following components,

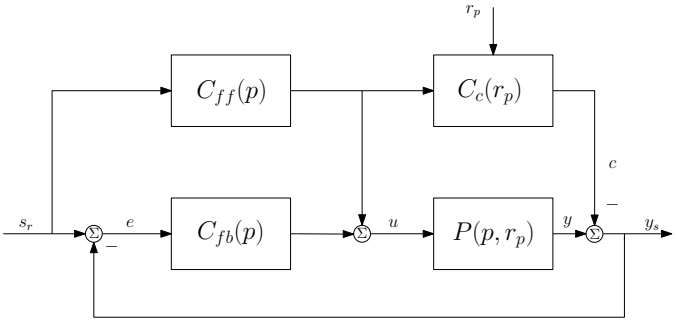

Fig. 2. Continuous compliance compensation control scheme. Since this block diagram contains time-varying dynamics, the *Laplace* variable s is replaced by the time differential operator, $p = \mathrm{d}/\mathrm{d}t$.

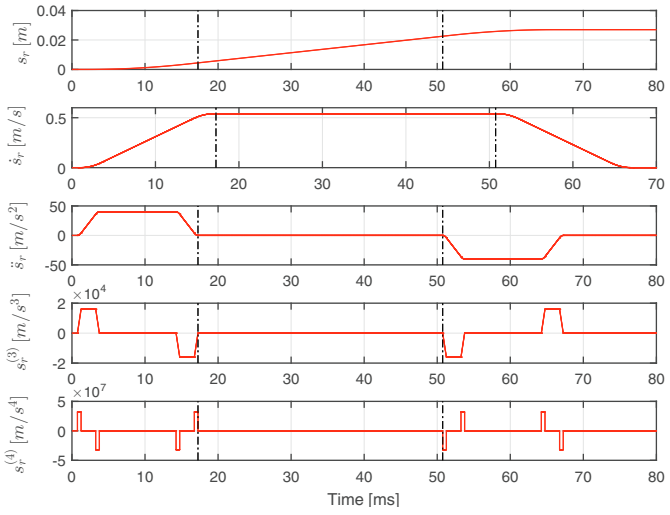

Fig. 3. Fourth-order reference setpoint s_r. The black dashed lines enclose the critical scanning interval (constant velocity).

(1) *Tracking setpoint:* The signal s_r is a fourth-order setpoint (see Fig. 3), which means that it is smooth up to its second derivative (acceleration), that is $s_r \in \mathcal{C}^3(0, \infty)$; note that the scanning interval of constant velocity (between the dashed lines) is the interval in which the tracking error is required to be small.
(2) *Plant:* The plant $P(p, r_p)$ is defined by either a finite or infinite-dimensional Single-Input Single-Output (SISO) flexible motion system, whose output location can be static or time-varying in nature. The performance location function r_p denotes the point-of-interest with respect (see below), and p is the time differential operator $p = \mathrm{d}/\mathrm{d}t$.
(3) *Feedback controller:* The Linear Time-Invariant (LTI) feedback controller $C_{fb}(s)$ (or $C_{fb}(p)$ in the time domain) acts on the error e between the setpoint and the plant output.
(4) *Performance location function:* In the case of position-dependent dynamics, which is considered in Section 3, a real function r_p is required, which indicates the performance location as a function of time $t \in \mathbb{R}$. For a distributed parameter system, we take $r_p \in \mathcal{C}^1$.

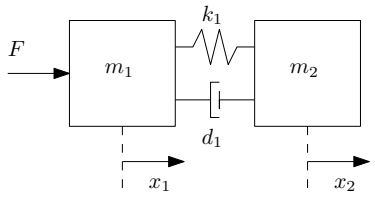

Fig. 4. Two mass-spring-damper system.

(5) *2-DOF feedforward controller:* The feedforward controller consists of two blocks, C_{ff} and C_c. C_{ff} filters the setpoint. Its output is split into two paths. One path enters the plant and the other path enters the second block C_c. In this work, the block C_{ff} is defined by a straightforward acceleration (mass) feedforward, that is

$$C_{ff}(s) = K_{fa}s^2 = Ms^2, \tag{1}$$

where M is the total mass of the system, K_{fa} the acceleration feedforward coefficient, and s the *Laplace* variable. The second block $C_c = C_c(r_p)$ denotes the so-called compliance compensation block. This block depends on the performance location function $r_p(t)$. It can be seen that the output of C_{ff} directly influences the control effort u, while the output of C_c manipulates the sensor output y, which through the feedback controller has an indirect influence.

The compliance compensation block C_c is a possibly time-varying memoryless gain, i.e. $C_c(t) \in \mathbb{R}$, and has a non-zero input and output only when there is non-zero acceleration or deceleration, see Fig. 3. The role of C_c is to mask the deformation of the flexible structure (plant P) during acceleration and deceleration phases by manipulating the plant output. The aim is to prevent the feedback controller from acting on the error otherwise occurring. This is because during acceleration and deceleration the error is not directly limiting performance, but the transient response otherwise induced by the feedback controller can well prolong into the scanning interval and thus become performance limiting.

To illustrate this, assume a finite order (lumped parameter) motion system, e.g. the two mass-spring-damper system shown in Fig. 4. Actuation occurs via a force $F(t)$ applied on the first mass. Naturally, the collocated and non-collocated response of the system are given by assuming as the point of interest either the displacement of the first mass $x_1(t)$ or the second mass $x_2(t)$, respectively. Solving the equations of motion for the non-collocated case and taking its *Laplace* transform, the transfer function is derived as

$$\frac{x_2(s)}{F(s)} = \underbrace{\frac{1}{Ms^2}}_{\text{RB mode}} + \underbrace{\frac{-m_1m_2}{M(m_1m_2s^2 + d_1Ms + k_1M)}}_{\text{NRB mode}}, \tag{2}$$

where m_1, m_2 are the two masses, k_1 the stiffness of the spring, d_1 the damping coefficient, and $M = m_1 + m_2$.

The frequency response of the system is decomposed in its rigid body (RB) and non-rigid body (NRB) mode components, as shown in (2). The NRB mode dynamics can in turn be divided into two parts, based on the frequency range of interest, namely the *compliant dynamics* and the *resonant dynamics*. This is shown in Fig. 5. As can be seen, the *compliant dynamics* (or simply compliance) are constant-valued, and equal the (static) response of the dynamics at the zero frequency. The compliance of the transfer function in (2) reads,

Spec.	Value
Mass 1	$m_1 = 0.2325$ [kg]
Mass 2	$m_2 = 0.2325$ [kg]
Spring constant	$k_1 = 6.03\,10^6$ [kg/m]
Damping coefficient	$d_1 = 10^{-3}$ [kg·sec/m]

Table 1. Mass-spring-damper system specifications.

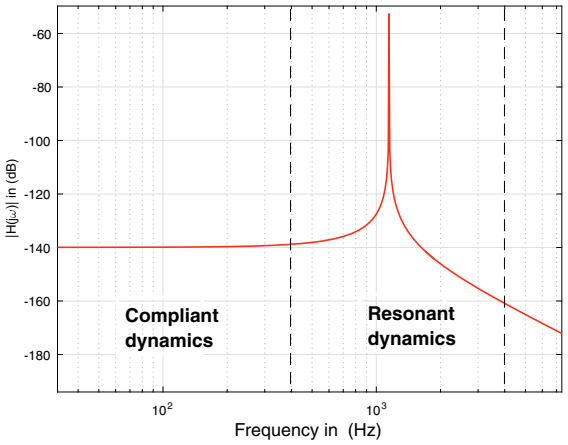

Fig. 5. Division of a flexible mode into its compliant and resonant dynamics.

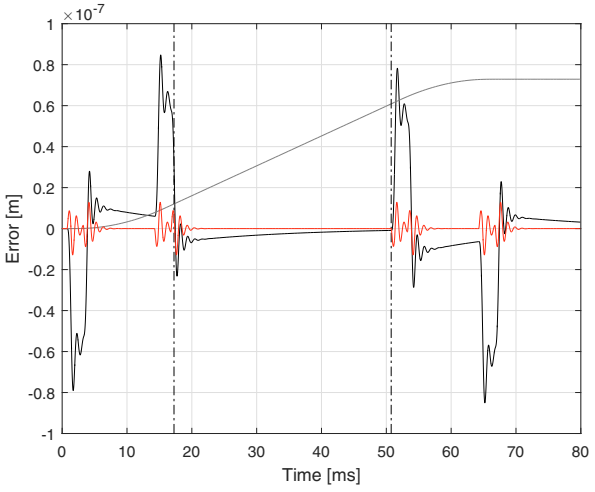

Fig. 6. Compliance compensation illustration, when tracking the fourth-order setpoint s_r in Fig. 3. The initial position of the motion system is assumed to be zero. The black and red lines depict the tracking error when acceleration (mass) feedforward is applied to the two mass-spring-damper system, with and without compliance compensation, respectively. The grey line depicts the (scaled) setpoint, and the vertical dashed lines enclose the constant-velocity (scanning) interval of the setpoint.

$$C_{msd} = \frac{-m_1 m_2}{k_1 M^2}. \tag{3}$$

The compliance compensation scheme considered in Fig. 2 can accurately compensate for the RB mode of the plant P plus its compliance. For the two mass-spring-damper system, this low-frequency approximation of the original plant can be written as

$$P_c(s) = \frac{1}{Ms^2} + C_{msd}. \tag{4}$$

Given (4), it can easily be seen that zero error is achieved when,

$$C_c = C_{msd}. \tag{5}$$

That is, the compliance compensation block is chosen to be equal to the compliance of the plant P; this holds not only for the two mass-spring-damper case, but in general.

The simulation results in Fig. 6 illustrate the performance benefits of compliance compensation, when applied to a two mass-spring-damper system whose specifications can be found in Table 1, with feedback controller

$$C_{\text{fb}}(s) = C_{\text{PID}}(s) C_1(s) N_1(s), \tag{6}$$

where

$$C_{\text{PID}}(s) = \frac{4.48\,10^8 s^2 + 3.26\,10^{10} s + 5.27\,10^{11}}{s}, \tag{7}$$

$$C_1(s) = \frac{1}{s + 3.168\,10^5}, \tag{8}$$

and notch filter,

$$N_1(s) = \frac{s^2 + 0.007124\,s + 5.187\,10^7}{s^2 + 1.296\,10^4 s + 5.187\,10^7}. \tag{9}$$

Additionally, the initial position of the motion system is assumed to be zero, which means that the initial condition for the error is also zero. It can be seen in Fig. 6 that masking of the error during acceleration and deceleration (red curve) prevents the feedback controller from reacting, which in the absence of the compliance compensation (black curve) causes transient settling effects induced by integral feedback which deteriorate the performance during the exposure interval.

In the next section, the compliance compensation scheme is extended to include the case of a time-varying point of interest and an infinite-dimensional (distributed parameter) system.

3. COMPLIANCE COMPENSATION OF DISTRIBUTED PARAMETER SYSTEMS

The transfer function that fully describes a distributed parameter system is naturally of infinite-order. Calculating a spatially continuous compliance function by exploiting the frequency response of this infinite-dimensional system is the purpose of this section.

Consider the homogeneous thin Euler-Bernoulli beam shown in Fig. 7. We denote the position of the beam r, the length L, the second moment of area I, the area A, the Young's modulus E, and the linear mass density ρ. The deflection of the beam at position r is $y(t,r)$, and there are no transverse forces applied to the element. Additionally, Kelvin-Voigt damping is added to the beam (Herrmann (2008)), where c_d denotes the damping coefficient. As can

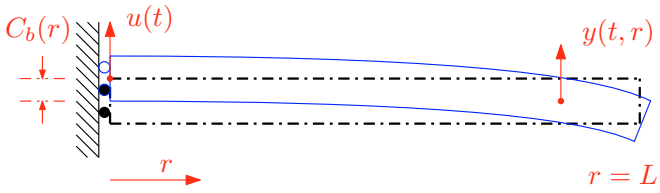

Fig. 7. Vertically-moving cantilever Euler-Bernoulli beam, where $u(t)$ the actuation force, $y(t,r)$ the displacement at the point-of-interest r, and L the length of the beam. A constant input force $u(t)$ results in a time-invariant deflection $C_b(r)$, which gives the compliance function of the beam.

be found in Moheimani et al. (2003), the PDE describing the beam system is given by

$$EI\frac{\partial^4 y(t,r)}{\partial r^4} + \rho A \frac{\partial^2 y(t,r)}{\partial t^2} + c_d \frac{\partial^5 y(t,r)}{\partial t \partial r^4} = 0. \tag{10}$$

As can be seen in Fig. 7, the beam is cantilever on one end, it is free at the other end, and actuation occurs through $u(t)$, which can be force or displacement. In this work, the input $u(t)$ defines a transverse force $F(t,r)$ exerted at the base of the beam, that is

$$F(t,0) = u(t). \tag{11}$$

The boundary conditions and PDE of the beam can be brought to the frequency domain via the *Laplace* transform. This enables the solution of the PDE, yielding the position-dependent transfer function of the beam, and which reads,

$$G_d(s,r) = \frac{f(r) + p_1(L-r,L) + p_2(L-r,L)}{A^{3/4}\rho^{3/4}s^{3/2}(-EI - c_d s)^{1/4}(k_1(L) + k_2(L))}, \tag{12}$$

where

$$\begin{aligned}
&1)\ p_1(x,y) = g(x,y) + g(y,x),\\
&2)\ p_2(x,y) = h(y,x) - h(x,y),\\
&3)\ f(x) = \cos(x\tilde{s}) + \cosh(x\tilde{s}),\\
&4)\ g(x,y) = \cos(x\tilde{s})\cosh(y\tilde{s}),\\
&5)\ h(x,y) = \sin(x\tilde{s})\sinh(y\tilde{s}),\\
&6)\ k_1(x) = \cos(x\tilde{s})\sinh(x\tilde{s}),\\
&7)\ k_2(x) = \sin(x\tilde{s})\cosh(x\tilde{s}), \quad \text{and}\\
&8)\ \tilde{s} = \frac{A^{1/4}\rho^{1/4}\sqrt{s}}{(-EI - c_d s)^{1/4}}.
\end{aligned} \tag{13}$$

Note that all functions in (13) depend on the *Laplace* variable s, however to ease notation explicit mention of s in the symbolism is omitted.

It can be seen that (12) is a non-rational transfer function. This is expected, as the beam is a distributed parameter system. Note that a force-to-position transfer function of a motion system generally contains a RB, and one or more NRB modes. In this case, the beam can be decomposed into an RB mode, and an infinite number of NRB modes, by taking a rational transfer function approximation of (12), (13).

Let us consider a modal approximation. An advantage of the modal approximation is that the mode decomposition is exact, that is, each structural mode's frequency and dynamics accurately reflect the beam, in contrast to e.g. a finite element model, where the resonance frequencies and dynamics only approximate the actual NRB modes of

the beam for increasing model order. Therefore, the term approximation refers to the need to consider up to a finite number of modes k, while neglecting the rest of the infinite modes comprising the beam. Given M_b the mass of the beam, its RB mode is given by,

$$G_{\mathrm{rb}}(s) = \frac{1}{M_b s^2} = \frac{1}{\rho A L s^2}. \tag{14}$$

Having laid the groundwork for the calculation of the continuous compliance function of the beam, we find an expression for the compliance. In the case of double integrator-based motion systems, the compliance C_{system} is found by the following limit,

$$C_{\mathrm{system}} = \lim_{s\to 0}\left(P(s) - \frac{1}{Ms^2}\right), \tag{15}$$

which is the total frequency response of the flexible components of the plant $P(s)$ when the frequency ω approaches zero, or equivalently when s approaches zero. Therefore, using (12)-(15), the position-dependent compliance of the beam can be calculated:

$$C_b(r) = \frac{6L^4 - 30L^2r^2 + 20Lr^3 - 5r^4}{120\,E\,I\,L}. \tag{16}$$

As can be seen, (16) gives the compliance of the beam, depending on the position r in a spatially continuous manner. The shape of the function denotes the deflection of the beam when accelerated (at the base) vertically by a constant force.

As a result of calculating the compliance function (16) of the distributed parameter system under consideration, compliance compensation for time-varying points of interest can be achieved easily. Namely, r is now given by a continuous-time function $r_p : I_p \to [0, L]$, where $I_p = [t_0, t_1] = \{t \in \mathbb{R} \,|\, t_0 < t < t_1\}$, which results in a time-dependent compliance function $C_b(r_p(t))$. Considering (1), (16), and the block diagram in Fig. 2, the output signal $c(t)$ of the compliance compensation block can be calculated as,

$$c(t) = C_b(r_p(t))\ddot{s}_r(t)\rho AL. \tag{17}$$

4. NUMERICAL EXAMPLE

The simulation results given in this section illustrate the continuous compliance compensation control scheme when applied to the beam system with a time-varying performance location. For the plant, a steel beam is considered, whose specifications can be found in Table 2. These specifications induce a frequency response that has similarities to a wafer stage, that is with respect to the RB and the first NRB mode's frequency and magnitude.

Spec.	Value
Length	$L = 0.6$ [m]
Cross-sectional area	$A = h^2 = 10^{-4}$ [m^2]
Mass density	$\rho = 7.75\,10^3$ [$\frac{\mathrm{kg}}{\mathrm{m}^3}$]
Young's modulus	$E = 2\,10^{10}$ [$\frac{\mathrm{kg}}{\mathrm{m}\,\mathrm{sec}^2}$]
Second moment of area	$I = \frac{h^4}{12} = \frac{10^{-4}}{12}$ [m^4]
Kelvin-Voigt damping	$c_d = 10^{-3}$

Table 2. Euler-Bernoulli beam specifications.

In frequency domain, the PDE describing this beam is given by,

$$\frac{d^4}{dr^4}Y(s,r) + \frac{2325}{3s + 5\,10^8}s^2Y(s,r) = 0. \tag{18}$$

The solution to (18) yields the position-dependent transfer function of the beam $G_d(s,r)$, as indicated in (12).

Since the beam is infinite-dimensional, a finite-order model is required for simulation purposes. The simulation model used here is based on the approximation employed to extract the RB mode from the infinite-dimensional transfer function of the beam, i.e. the modal approximation. For illustration purposes, only the first NRB mode of the beam will be considered, however, the modeling strategy remains valid if more than one NRB modes are included in the simulation model. Given a pole λ_k, we define $a = \mathrm{Re}(\lambda_k)$, $b = \mathrm{Im}(\lambda_k)$, $c(r) = \mathrm{Re}(Res(\lambda_k, r))$, $d = \mathrm{Im}(Res(\lambda_k, r))$, where $Res(\lambda_k, r)$ is the Cauchy residue of the pole λ_k (see Curtain, Morris (2009)), which is dependent on r. The first NRB mode of the beam is given by

$$\begin{aligned} G_1(s,r) =& \frac{Res(\lambda_1, r)}{s - \lambda_1} + \frac{Res(\lambda_1^*, r)}{s - \lambda_1^*} \\ =& \frac{2(c(r)s - ac(r) - bd(r))}{s^2 - 2as + a^2 + b^2}. \end{aligned} \tag{19}$$

Naturally the frequency response along the beam changes only through the residue, which affects only the zeros. The poles of the structure remain unchanged, regardless the point of interest.

From (19) it can be seen that the compliance of the single flexible mode is given by,

$$C_{\lambda_1}(r) = \lim_{s\to 0} G_1(s,r) = \frac{-2(a\,c(r) + b\,d(r))}{a^2 + b^2}. \tag{20}$$

Thus, the compliance of the beam will differ from this simulation model with one NRB mode. Therefore an adjustment in the compliance is required to correctly match the compliance to the infinite-dimensional beam system. The simulation model is given as follows,

$$G_{\mathrm{s}}(s,r) = G_{\mathrm{rb}}(s) + G_1(s,r) + C_b(r) - C_{\lambda_1}(r). \tag{21}$$

Simulations were performed in continuous time. The simulation model (21) was encapsulated into an LPV model, i.e. a smooth family of LTI systems. The griding of the LPV model was increased until improvements in the error became insubstantial (this occurred for a set of approximately two hundred LTI systems). The fourth-order trajectory s_r in Fig. 3 is used as the tracking setpoint, while the time-varying point-of-interest trajectory r_p was chosen as the function

$$r_{\mathrm{p}}(t) = 0.3\,(1 - \cos(12.5\pi t))\,, \tag{22}$$

which scans the whole beam from the base toward the end, since $r(t) \in [0, 0.6]$, with period $T = 160$ [ms]. Given this time-function r_p results in the following time-varying system,

$$G_{\mathrm{s}}(p, r_p) = G_{\mathrm{rb}}(p) + G_1(p, r_p) + C_b(r_p) - C_{\lambda_1}(r_p). \tag{23}$$

The feedback controller, which robustly stabilizes the beam in the case that one or two NRB modes are included in the model, irrespective of the position r considered, is given by

$$C_{\mathrm{fb}}(s) = C_{\mathrm{PID}}(s)C_{1\mathrm{st}}(s)N_1(s)N_2(s)N_{\mathrm{s}}(s), \tag{24}$$

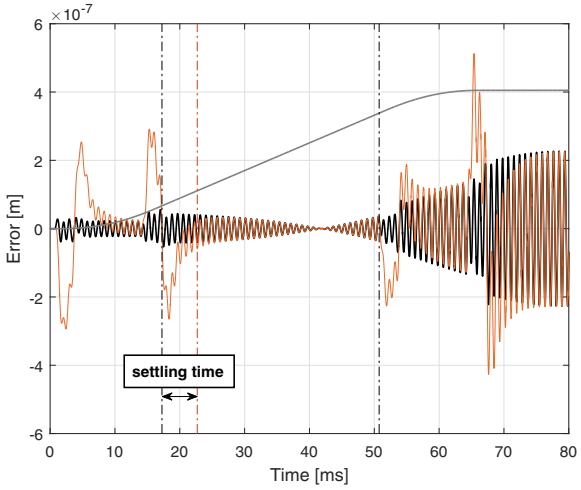

Fig. 8. Simulation with (black) and without (red) compliance compensation for the beam with a time-varying performance location, in closed loop. The scanning interval is enclosed by the vertical dashed lines, while the (scaled) tracking setpoint is drawn in gray. The red line indicates the settling time caused by feedback transient effects when compliance compensation is not present.

where

$$C_{\mathrm{PID}}(s) = \frac{1.64\,10^{8}s^{2} + 6.48\,10^{10}s + 9.93\,10^{11}}{s}, \tag{25}$$

$$C_{\mathrm{1st}}(s) = \frac{1}{s + 2.088\,10^{5}}, \tag{26}$$

$$N_{1}(s) = \frac{s^{2} + 0.3184\,s + 5.191\,10^{7}}{s^{2} + 1.297\,10^{4}s + 5.191\,10^{7}}, \tag{27}$$

$$N_{2}(s) = \frac{s^{2} + 8.823\,s + 1.516\,10^{9}}{s^{2} + 7.008\,10^{4}s + 1.516\,10^{9}}, \tag{28}$$

and

$$N_{\mathrm{s}}(s) = \frac{6.25\,10^{-6}s^{2} + 7.226\,s + 2.088\,10^{8}}{s^{2} + 2890s + 2.088\,10^{8}}. \tag{29}$$

The simulation results are shown in Fig. 8, which shows the tracking error with (black) and without (red) compliance compensation. It can be seen that the accurate prediction of the compliance masks the error, preventing the feedback controller from inducing transient phenomena into the scanning interval. In this particular case, assuming a settling error threshold of 50 [nm], absence of compliance compensation causes a settling time of approximately 5.5 [ms], which is substantial when compared to the total duration of the scanning interval, which is about 33.5 [ms]. Another observation regarding the simulation results is the general tendency of the error to increase with time. This is because through the choice of (22) the point of interest moves from the base of the beam toward the end of the beam, where the beam's vibrations are much more pronounced.

5. CONCLUSIONS AND REMARKS

This paper discusses a compliance compensation control scheme for flexible structures with time-varying performance locations. The PDE of an Euler-Bernoulli beam with Kelvin-Voigt damping was exploited in order to derive the closed form of the position-dependent compliance function for the beam. Simulations using a fourth-order setpoint trajectory and an arbitrary point-of-interest time function indicate accurate compliance estimation for the beam, and thus improved performance in terms of overshoot and settling times.

REFERENCES

Moheimani, S.O.R., Halim, D., and Fleming, A.J. (2003). *Spatial Control of Vibration*, World Scientific.

Herrmann, L. (2008). *Vibration of the Euler-Bernoulli Beam with Allowance for Dampings*, Lecture Notes in Engineering and Computer Science, vol. 2078, pp. 901-904.

Curtain, R., and Morris, K. (2009). *Transfer Functions of Distributed Parameter Systems: A Tutorial*, Automatica, vol. 45, issue 5, ISSN 0005-1098, pp. 1101-1116.

Moore, G.E. (1965). *Cramming more components on integrated circuits*, Electronics, vol. 38, no. 8, pp. 1–3.

Boerlage, M. (2006). *MIMO jerk derivative feedforward for motion systems*, in American Control Conference, pp. 3892–3897.

Ronde, M.J.C., Schneiders, M.G.E., van de Molengraft, M.J.G.R., de Haas, D., and Steinbuch, M. (2012). *Spatial feedfoward for over-actuated flexible motion systems*, in The 13th Mechatronics Forum International Conference, R. Scheidl and B. Jakoby, Eds., vol. 1/3. Linz: Trauner- Verlag, pp. 254–260.

Lambrechts, P., Boerlage, M., and Steinbuch, M. (2005). *Trajectory planning and feedforward design for electromechanical motion system*, Control Engineering Practice, vol. 13, no. 2, pp. 145–157.

Ronde, M., van den Bulk, J., van de Molengraft, M.J.G.R., and Steinbuch, M. (2013). *Feedforward for flexible systems with time-varying performance locations*, in American Control Conference, 2013 , vol. 23, no. 4, , pp. 6033-6038.

Dijkstra, B.G. (2004). *Iterative Learning Control with applications to a wafer stage*, PhD thesis, Technische Universiteit Delft.

van de Wijdeven, J.J.M. (2008). *Iterative Learning Control design for uncertain and time-windowed systems*, PhD thesis, Eindhoven University of Technology.

Oomen, T., Grassens, E., Hendriks, F. (2015). *Inferential Motion Control: Identification and Robust Control Framework for Positioning an Unmeasurable Point of Interest*, IEEE Transactions on control systems technology, vol. 23, no. 4, pp. 1602-1610.

Sato, M. (2003). *Gain-scheduled inverse system and filtering system without derivatives of scheduling parameters*, in American Control Conference, vol. 5, pp. 4173-4178.

Sato, M. (2008). *Inverse system design for LPV systems using parameter-dependent Lyapunov functions*, Automatica, vol. 44, issue 4, pp. 1072-1077.

Vervoordeldonk, M.J., Baggen, M.C.J. (2009). *Position control system, a lithographic apparatus and a method for controlling a position of a movable object* , USPTO, 20090268185-A1.